Korean J. Chem. Eng., **24**(3), 397-402 (2007)

Synthesis of nanocrystalline alumina by thermal decomposition of aluminum isopropoxide in 1-butanol and their applications as cobalt catalyst support

Kamonchanok Pansanga, Okorn Mekasuwandumrong*, Joongjai Panpranot and Piyasan Praserthdam†

Center of Excellence on Catalysis and Catalytic Reaction Engineering, Department of Chemical Engineering, Faculty of Engineering, Chulalongkorn University, Bangkok 10330, Thailand
*Department of Chemical Engineering, Faculty of Engineering and Industrial Technology, Silpakorn University, Nakorn Pathom 73000, Thailand
(*Received 21 August 2006 • accepted 13 November 2006*)

Abstract−Nanocrystalline alumina powders were prepared by thermal decomposition of aluminum isopropoxide (AIP) in 1-butanol at 300 °C for 2 h and employed as cobalt catalyst supports. The crystallization of alumina was found to be influenced by the concentration of AIP in the solution. At low AIP content, wrinkled sheets-like structure of γ-Al_2O_3 was formed, while at high AIP concentrations, fine spherical particles of χ-Al_2O_3 were obtained. It was found that using these fine particles alumina as cobalt catalyst supports resulted in much higher amounts of cobalt active sites measured by H_2 chemisorption and higher CO hydrogenation activities.

Key words: Nanocrystalline Alumina, Thermal Decomposition, Cobalt Catalyst, Solvothermal Method, CO Hydrogenation

INTRODUCTION

Alumina powders are very interesting crystalline materials with broad applicability as adsorbents, coatings, soft abrasives, ceramic tools, fillers, wear-resistant ceramics, catalysts, and catalyst supports [1,2]. Because of their fine particle size, high surface area, high melting point (above 2,000 °C), high purity, good adsorbent, and high catalytic activity, they have been employed in a wide range of large-scale technological processes [3,4].

Various transition aluminas (α, γ, χ, δ, η and θ) have been prepared by different methods, such as sol-gel synthesis [5,6], hydrothermal synthesis [7], microwave synthesis [8], emulsion evaporation [9], plasma technique [10], and solvothermal synthesis [11-18]. Among these methods, solvothermal synthesis attracts the most attention because it gives the products with small uniform morphology, well-controlled chemical composition, and narrow size distribution. Furthermore, the desired shape and size of particles can be produced by controlling process conditions such as solute concentration, reaction temperature, reaction time, and the type of solvent [19,20]. For example, Berntsen et al. [21] described a simple route to high surface area nanostructured MoS_2 based on the decomposition of cluster-based precursor $(NH_4)_2Mo_3S_{13}\cdot xH_2O$ in toluene at 380 °C. It was found that solvothermal decomposition resulted in nanostructured material distinct from that obtained by decomposition of the precursor in sealed quartz tubes at the same temperature. Wang et al. [22] prepared nanocrystalline titania in alcohols under solvothermal conditions at 100 °C for 24 h. The selection of crystal structures, grain sizes, and morphologies was achieved by simply varying the alcohols and other reaction conditions.

Alumina prepared by the solvothermal method is considered high thermal stability. In our recent works [23-26], nanocrystalline transition alumina with micro spherical particles and high thermal stability has been synthesized by decomposition of aluminum isopropoxide (AIP) under solvothermal conditions. The mechanism of the process involves the formation of amorphous complexes before further decomposition takes place. Inoue et al. [27] prepared silica-modified alumina by the reaction of AIP and tetraethyl orthosilicate (TEOS) in 1,4-butanediol at 300 °C. The products were found to maintain large surface areas after calcination at high temperature.

In this study, the influence of concentration of aluminum isopropoxide in 1-butanol used in the preparation of nanocrystalline alumina by solvothermal method on the properties of alumina powders and alumina supported cobalt catalysts was investigated by using various characterization techniques such as XRD, BET analysis, TEM, SEM, EDX, H_2 chemisorption, and temperature-programmed reduction. The catalytic activity of the catalysts was tested in carbon monoxide hydrogenation at 220 °C and atmospheric pressure.

EXPERIMENTAL

1. Catalyst Preparation

1-1. Preparation of Nanocrystalline Al_2O_3

A selected amount of aluminum isopropoxide (Aldrich) (10-35 g) was suspended in 100 ml of 1-butanol (Ajax Finechem) in a test tube, which was then placed in a 300 ml autoclave. In the gap between the test tube and the autoclave wall, 30 ml of 1-butanol was added. The atmosphere inside the autoclave was purged completely with nitrogen. The mixture was heated to 300 °C at a heating rate of 2.5 °C/min and was kept at that temperature for 2 h. After cooling to room temperature, the resulting powders were collected after repeated washing with acetone by centrifugation. They were then air-dried. The calcination of the products was carried out in a box furnace by heating up to 600 °C at a rate of 10 °C/min and held at that temperature for 1 h.

1-2. Preparation of Al_2O_3-Supported Co Catalysts

The Co/Al_2O_3 catalysts were prepared by incipient wetness impregnation of Al_2O_3 with a desired amount of an aqueous solution

†To whom correspondence should be addressed.
E-mail: piyasan.p@chula.ac.th

of cobalt nitrate [$Co(NO_3)_2 \cdot 6H_2O$] (Aldrich). The final loading of the catalysts was determined by atomic absorption spectroscopy (Varian Spectra A800) to be ca. 10 wt% cobalt. The catalysts were dried at 110 °C for 24 h and calcined in air at 300 °C for 2 h using a ramp rate of 1 °C/min.

2. Catalyst Nomenclature

In this study, alumina and alumina-supported cobalt catalysts are referred to as Al-x and Co/Al-x, where x is the amount (g) of AIP used in the preparation of alumina powders. For example, Al-10 and Co/Al-10 refer to Al_2O_3 and Co/Al_2O_3 catalyst prepared with 10 g AIP.

3. Catalyst Characterization

XRD patterns of the samples were collected with a SIEMENS D-5000 X-ray diffractometer with Cu K_α radiation (λ=1.54439 Å). The spectra were scanned at a rate of 0.04°/step from 2θ=15° to 80°. BET surface areas were calculated by using the BET-single point method at liquid N_2 temperature. Transmission electron microscopy (TEM) was performed with a JEOL JEM1220. SEM and EDX were performed with a JEOL JSM-35CF scanning electron microscope in the back scattering electron (BSE) mode at 20 kV. EDX was performed by using Link Isis 300 software. Static H_2 chemisorption was carried out on the reduced cobalt catalyst samples at 100 °C according to the method described by Reuel and Bartholomew [28] by using a Micromeritics Pulse Chemisorb 2700 system. Prior to H_2 chemisorption, the catalyst samples were reduced at 350 °C in flowing H_2 for 3 h. Temperature-programmed reduction (TPR) was performed by using an in-house system. Approximately 0.1 g of the catalyst was placed in the middle of a stainless steel reactor. A temperature ramp from 35 to 600 °C at a ramp rate 5 °C/min and the reduction gas 5% H_2 in Ar were used. A thermal conductivity detector (TCD) was used to determine the amount of hydrogen consumed. A cold trap was placed before the detector to remove water produced during the reduction. The hydrogen consumption was calibrated by using TPR of silver oxide (Ag_2O) at the same conditions.

4. Reaction

CO hydrogenation was carried out in a fixed-bed quartz reactor under differential reaction conditions (<10% conversion) at 220 °C, 1 atm total pressure, and H_2/CO=10/1. The total flow rate of H_2/CO/Ar was 80/8/32 cc/min. Typically, 0.1 g of the catalyst sample was reduced *in situ* in flowing H_2 (50 cc/min) at 350 °C for 3 h prior to CO hydrogenation. After the startup, samples were taken in 1-h interval and analyzed by gas chromatography. Steady state was reached within 6 h in all cases.

RESULTS AND DISCUSSION

1. Effect of AIP Concentration on the Properties of Al_2O_3

Fig. 1 shows the XRD patterns of various alumina powders obtained from thermal decomposition of AIP in 1-butanol after calcination at 600 °C for 1 h. XRD patterns of Al_2O_3 show strong diffraction peaks at 31°, 33°, 38°, 43°, 47.5°, and 68° (according to the JCPDSs database). It was found that when lower amounts of AIP were used, only γ-alumina was formed as seen by the XRD characteristic peaks at 2θ=33° according to the JCPDSs database. The XRD characteristic peaks of χ-alumina were observed at 2θ=42.5° for the ones prepared with AIP 25 and 35 g. The intensity of χ-alumina peaks became stronger with increasing amount of AIP content. It is indicated that increasing AIP content during the synthesis resulted in formation of mixed phase between γ-alumina and χ-alumina. The crystallization process of alumina was probably affected by the amounts of AIP in 1-butanol.

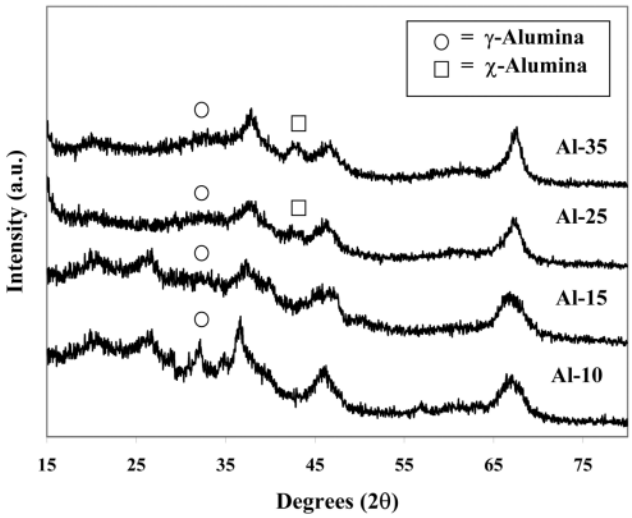

Fig. 1. XRD patterns of various nanocrystalline alumina prepared by the reaction of AIP in 1-butanol at 300 °C for 2 h (after calcinations at 600 °C for 1 h).

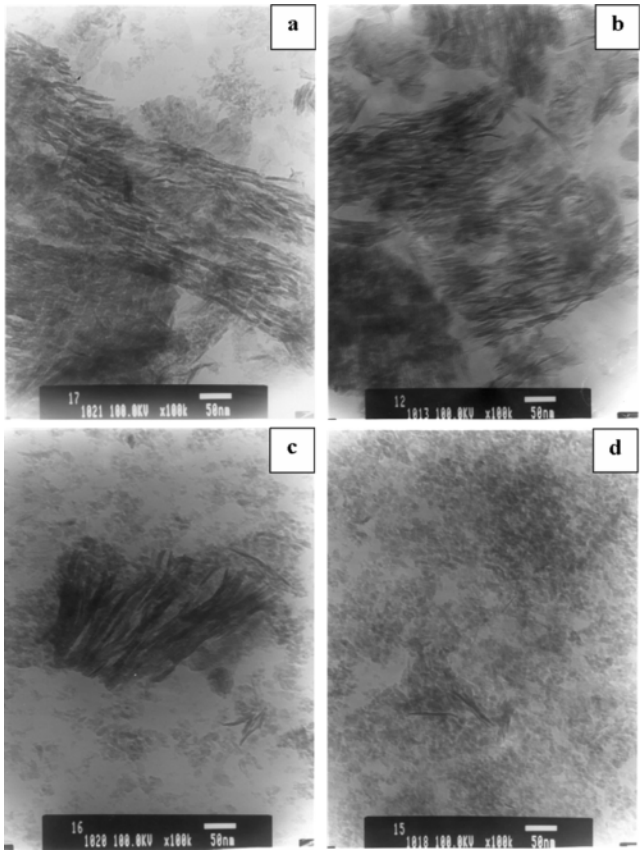

Fig. 2. TEM images of alumina obtained by the reaction of AIP in 1-butanol at 300 °C for 2 h with different amounts of AIP (a) Al-10 (b) Al-15 (c) Al-25 (d) Al-35.

Table 1. The physical and chemical properties of Al_2O_3 supports

Samples	Amounts of AIP (g)	Surface area (m^2/g)[a]	Bulk density (g/cm^3)[a]	Morphology
Al-10	10	70	0.3824	Wrinkled sheets
Al-15	15	120	0.3858	High amount of wrinkled sheets
Al-25	25	139	0.3928	Wrinkled sheets and small amount of spherical particles
Al-35	35	145	0.5358	Small amount of wrinkled sheets and high amount of spherical particles

[a]Error of measurement=±5%

TEM images of alumina powders prepared with different amounts of AIP are shown in Fig. 2. For the ones prepared with lower amounts of AIP, Al-10 and Al-15, the wrinkled sheets morphology was observed. They were found to be similar to those obtained from the formation of γ-alumina by decomposition of glycol or alkyl derivatives on boehmite [26,27]. As the amounts of AIP increased, the wrinkled sheets morphology became less apparent and spherical particles were observed. The presence of spherical particles was probably due to the formation of χ-alumina, which is normally formed by thermal decomposition reaction of AIP in inert organic solvents at 300 °C [23-26]. TEM results were in good agreement with the XRD patterns that a mixture of γ-alumina and χ-alumina was observed when AIP concentration increased.

The physical properties of the alumina products are summarized in Table 1. The BET surface areas increased with increasing AIP concentration as a result of morphology changing from wrinkled sheets structure to small spherical particles. BET surface area of the Al-35 (145 m^2/g) was found to be twice of that of Al-10 (70 m^2/g). Similar trend was observed for the bulk density of the alumina powders. The bulk density increased with increasing AIP contents.

Mechanism of thermal decomposition of AIP in alcohol has been proposed in our previous works [23,26] involving three competitive reactions. First, AIP reacted with 1-butanol yielding aluminum butoxide, which decomposed further to give the alkyl (butyl) derivative of boehmite. Second, 1-butanol can be dehydrated to give water which then hydrolyzes aluminum isopropoxide or butoxide yielding pseudoboehmite. Finally, the direct decomposition of aluminum alkoxide in organic solvent, which proceeded slowest, gave χ-alumina. In the present work, at low AIP content, boehmite was probably the main product and γ-alumina was obtained after calcination at 600 °C for 1 h. The morphology of the boehmite products obtained via solvothermal reaction was wrinkled sheets [23,26], which was also similar to those of γ-alumina decomposed from. However, when the amounts of AIP in 1-butanol increased, formation of χ-alumina from direct decomposition of AIP in the solvent occurred as the main reaction.

2. Characteristics of Co/Al_2O_3 Catalysts

The XRD patterns of cobalt catalysts supported on alumina prepared with various amounts of AIP are shown in Fig. 3. The XRD patterns of the Co/Al_2O_3 catalysts were not significantly different from those of alumina supports. No XRD peaks of Co_3O_4 or other Co compounds were detected. This indicates that cobalt was present in a highly dispersed form on alumina even for cobalt loading as high as 10 wt% [29].

SEM and EDX were performed in order to study the morphology and elemental distribution of the catalyst samples, respectively. Typical SEM micrographs of Co/Al_2O_3 catalysts are shown in Fig. 4. There was no significant change in morphology of the catalyst samples due to the effect of AIP concentrations in 1-butanol used in the preparation process. The white or light spots observed in all figures can be attributed to the cobalt patches distributed on the external surface of catalyst granules. Fig. 5 shows the SEM micrographs and the EDX mapping of the cross-sectioned Co/Al-35 catalyst granule. The distribution of cobalt was found to be well dispersed throughout the catalyst granule.

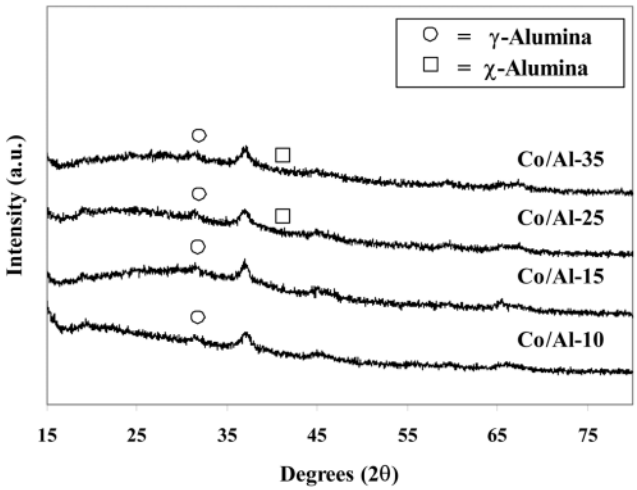

Fig. 3. XRD patterns of Co/Al_2O_3 catalysts with different amounts of AIP.

The relative amounts of active surface cobalt on the catalyst samples were calculated from H_2 chemisorption experiments at 100 °C according to Reuel and Bartholomew [28]. It is known that only surface cobalt metal atoms are active for CO hydrogenation, not its oxide or carbide [30]. The H_2 chemisorption results are reported in Table 2. The amounts of H_2 chemisorption increased from 0.90 to 20.65 μmol/g cat., with increasing amount of AIP in 1-butanol used in the preparation of the alumina supports from 10 to 35 g. It is likely that the increase in the relative amounts of active cobalt metals was due to the formation of the small spherical particles of χ-alumina. As also seen in the Table 2, the amount of H_2 chemisorption of Co/Com-Al (13.38 μmol/g cat.), prepared from the commercial γ-alumina which the crystal shape of alumina was spherical (the results was not shown), was better than solvothermal-made Co/γ-alumina (0.90 μmol/g cat.) but lower than Co/χ-alumina (20.65 μmol/g cat.).

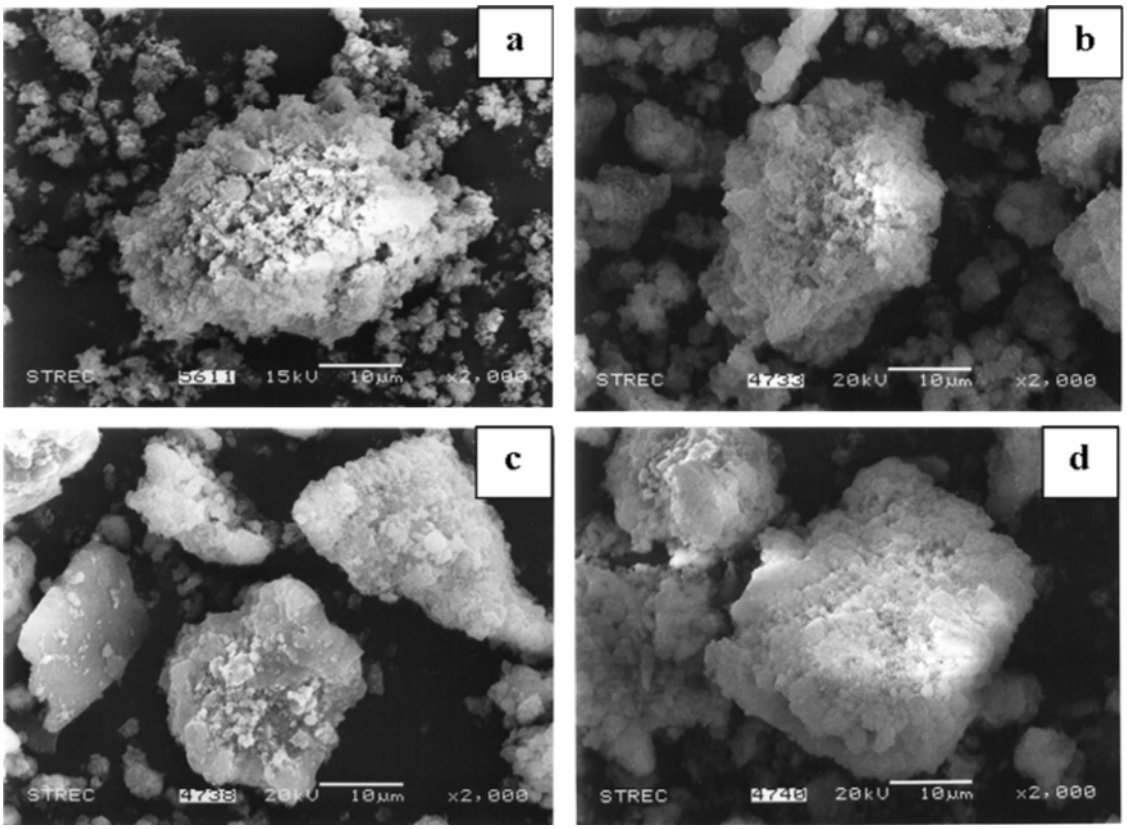

Fig. 4. SEM micrographs of (a) Co/Al-10, (b) Co/Al-15, (c) Co/Al-25, and (d) Co/Al-35.

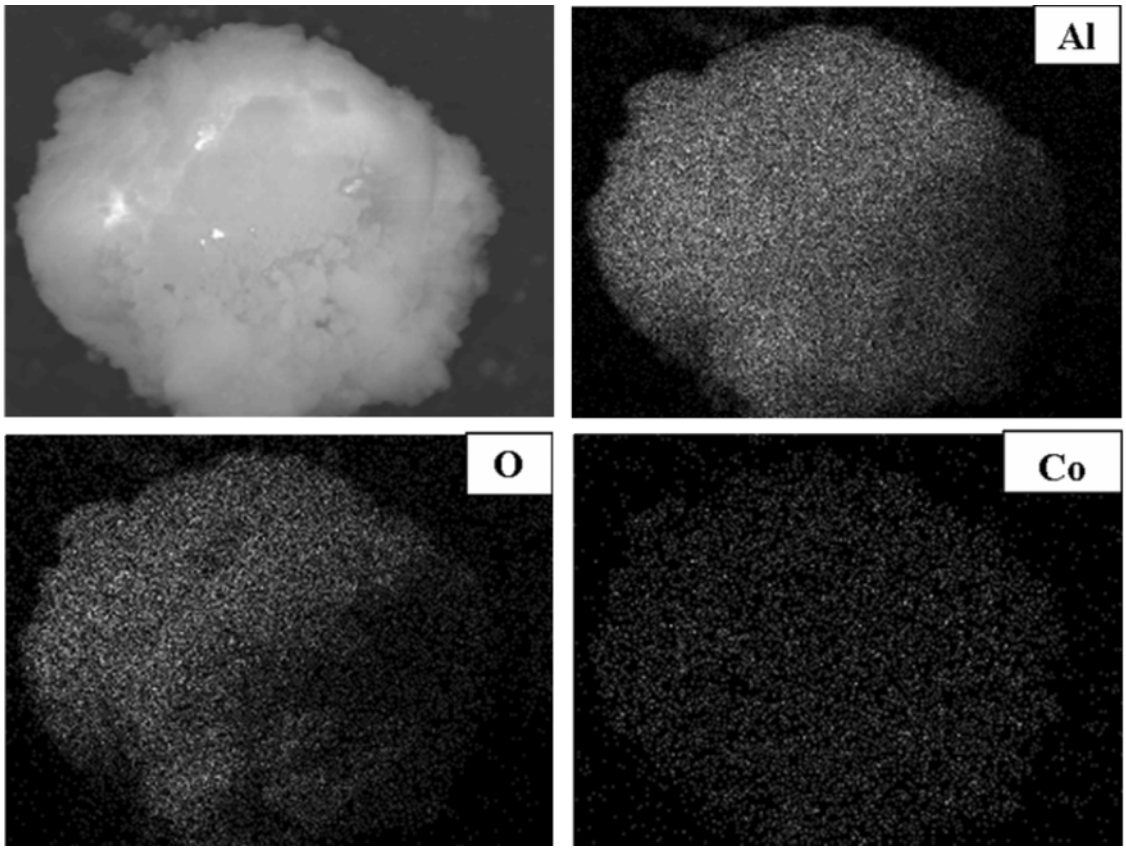

Fig. 5. SEM micrograph and EDX mapping of cross-sectioned Co/Al-35 catalyst granule.

It was again confirmed that the spherical morphology of the alumina support is important in achieving a higher amount of active cobalt metal.

3. Reduction and Catalytic Behaviors of Co/Al_2O_3 Catalysts

Temperature program reduction (TPR) is a powerful tool for studying the reduction behavior of the catalysts. The TPR profiles of various nanocrystalline alumina supported cobalt catalysts are shown in Fig. 6. All the catalyst samples exhibited two main reduction peaks which could be assigned to the two-step reduction of Co_3O_4: first reduction of Co_3O_4 to CoO and then the subsequent reduction of CoO to Co^0 [31]. The two reduction steps may not always be observed as separate peaks in TPR profile [32], as seen in the Co/Al-35 sample. A wide range of variables such as metal particle size and metal-support interaction have an influence on the reduction behavior of cobalt catalysts resulting in the observation of different locations of the TPR peaks. The TPR profiles for all the catalysts except Co/Al-35 appeared to be not significantly different, suggesting that the AIP content had little impact on the interaction of cobalt and alumina supports. Thus, high dispersion of cobalt obtained on Co/Al-35 was rather to be due to the formation of small spherical particles alumina and not to the change in reducibility of the catalysts.

Table 2. The characteristics and H_2 chemisorption of cobalt catalyst

Catalyst samples	Surface area (m^2/g)[a]	Amount of H_2 chemisorption ($\mu mol/g$ cat.)[a]
Co/Al-10	61	0.90
Co/Al-15	87	2.29
Co/Al-25	108	7.58
Co/Al-35	114	20.65
Co/Com-Al*	145	13.38

[a]Error=±5%, as determined directly.
*Commercial γ-alumina, BET surface area of alumina 230 m^2/g.

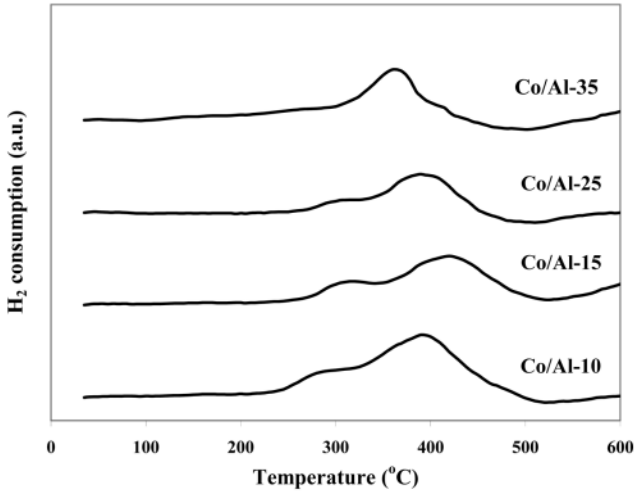

Fig. 6. TPR profiles of the catalyst samples.

CO hydrogenation reaction was carried out as a test reaction to determine the catalytic activity of the catalyst samples. The results are shown in Table 3. It is clearly seen that alumina prepared with higher amounts of AIP in 1-butanol resulted in much higher CO hydrogenation activities and CH_4 selectivities. The reaction results confirm the amount of surface cobalt metals measured by H_2 chemisorption.

CONCLUSIONS

Nanocrystalline alumina powders were prepared by thermal decomposition of AIP in 1-butanol with various AIP contents. The concentration of AIP in 1-butanol had a significant impact on the properties of alumina and alumina supported cobalt catalysts. Increasing amounts of AIP in the solution resulted in the transformation of wrinkled sheet γ-alumina to fine spherical particles of χ-alumina. It also gave rise to the cobalt active sites and CO hydrogenation activities when employed as supports for preparation of Co/Al_2O_3 catalysts.

ACKNOWLEDGMENTS

The authors would like to thank the Thailand Research Fund (TRF) for the financial support of this project.

REFERENCES

1. J. S. Church, N. W. Cant and D. L. Trimm, *Appl. Catal. A*, **101**(1), 105 (1993).
2. G. Pajonk and S. Teichner, *Aerogels*, Spinger, Berlin (1986).
3. C. Misra, *Industrial alumina chemicals*, ACS Monograph 184, Washington (1986).

Table 3. Reaction rate and selectivity for CO hydrogenation on catalyst samples

Catalyst samples	CO conversion (%)[a]		Rate ($\times 10^2$ gCH_2 $gcat^{-1}h^{-1}$)[b]		CH_4 selectivity (%)	
	Initial[c]	SS[d]	Initial	SS	Initial	SS
Co/Al-10	1.92	0.54	5.76	1.62	13	11
Co/Al-15	2.63	0.75	7.89	2.25	49	47
Co/Al-25	5.45	3.02	16.35	9.06	56	54
Co/Al-35	8.49	4.03	25.47	12.09	70	67

[a]CO hydrogenation was carried out at 220 °C, 1 atm, and $H_2/CO/Ar=80/8/32$.
[b]Error±5%, as determined directly.
[c]After 20 min of reaction.
[d]After 6 h of reaction.

4. H. Topsoe, B. S. Clausen and F. E. Massoth, *Hydrotreating catalysis*, Springer, Berlin (1996).
5. C. J. Brinker and G. W. Scherrer, *Sol-gel science*, Academic Press, San Diego (1990).
6. K.-C. Song, K.-J. Woo and Y. Kang, *Korean J. Chem. Eng.*, **16**, 75 (1999).
7. W. H. Dawson, *Am. Ceram. Soc. Bull.*, **67**, 1673 (1988).
8 S. G. Deng and Y. S. Lin, *Sci. Lett.*, **16**, 1291 (1997).
9. Y. Sarikaya, I. Sevinc and M. Akinc, *Powder Technol.*, **116**(1), 109 (2001).
10. S.-M. Oh and D.-W. Park, *Korean J. Chem. Eng.*, **17**, 299 (2000).
11. M. Inoue, H. Kominami and T. Inui, *J. Am. Ceram. Soc.*, **73**, 1100 (1990).
12. M. Inoue, H. Kominami and T. Inui, *J. Chem. Soc. Dalton Trans.*, 3331 (1991).
13. M. Inoue, H. Kominami and T. Inui, T. *J. Am. Ceram. Soc.*, **75**, 2597 (1992).
14. M. Inoue, H. Kominami and T. Inui, *Appl. Catal. A*, **97**, L25 (1993).
15. M. Inoue, H. Kominami and T. Inui, *Appl. Catal. A*, **121**, L1 (1995).
16. M. Inoue, H. Kominami and T. Inui, *J. Am. Ceram. Soc.*, **75**, 2597 (1996a).
17. M. Inoue, Y. Kondo and T. Inui, *Inorg. Chem.*, **27**, 215 (1988).
18. M. Inoue, H. Otsu, H. Kominami and T. Inui, *Ind. Eng. Chem. Res.*, **35**, 295 (1996b).
19. Y. Deng, G-D. Wei and C.-W. Nan, *Chem. Phys. Lett.*, **368**(5-6), 639 (2003).
20. Y. Deng, X.-S. Zhou, G-D. Wei, J. Liu, C.-W. Nan and S.-J. Zhao, *J. Phys. Chem. Solids*, **63**(11), 2119 (2002).
21. N. Berntsen, T. Gutjahr, L. Loeffler, J. R. Gomm, R. Seshadri and W. Tremel, *Chem. Mater.*, **15**(23), 4498 (2003).
22. C. Wang, Z.-X. Deng, G. Zhang, S. Fan and Y. Li, *Powder Technol.*, **125**(1), 39 (2002.
23. O. Mekasuwandumrong, H. Kominami, P. Praserthdam and M. Inoue, *J. Am. Ceram. Soc.*, **87**(8), 1543 (2004a).
24. O. Mekasuwandumrong, P. Praserthdam, M. Inoue, V. Pavarajarn and W. Tanakulrungsank, *J. Mater. Sci.*, **39**, 2417 (2004b).
25. O. Mekasuwandumrong, P. L. Silveston, P. Praserthdam, M. Inoue, V. Pavarajarn and W. Tanakulrungsank, *Inorg. Chem. Commu.*, **6**(7), 930 (2003).
26. P. Praserthdam, M. Inoue, O. Mekasuvandumrong, W. Tanakulrungsank and S. Phatanasri, *Inorg. Chem. Commu.*, **3**(11), 671 (2000).
27. M. Inoue, H. Otsu, H. Kominami and T. Inui, *Ind. Eng. Chem. Res.*, **35**, 295 (1996c).
28. R. C. Reuel and C. H. Bartholomew, *J. Catal.*, **85**, 63 (1984).
29. B. Jongsomjit, J. Panpranot and J. G. Goodwin Jr., *J. Catal.*, **215**(1), 66 (2003).
30. R. B. Anderson, *The Fischer-Tropsch synthesis*, Academic Press, San Diego (1984).
31. Y. Zhang, D. Wei, S. Hammache and J. G. Goodwin Jr., *J. Catal.*, **188**(2), 281 (1999).
32. B. Ernst, S. Libs, P. Chaumette and A. Kiennemann, *Appl. Catal. A*, **186**(1-2), 145 (1999).